Wear 297 (2013) 1095–1102

Contents lists available at SciVerse ScienceDirect

Wear

journal homepage: www.elsevier.com/locate/wear

Transfer film evolution and its role in promoting ultra-low wear of a PTFE nanocomposite

J. Ye, H.S. Khare, D.L. Burris *

Department of Mechanical Engineering, University of Delaware, Newark, DE, United States

ARTICLE INFO

Article history:
Received 23 July 2012
Received in revised form
23 November 2012
Accepted 6 December 2012
Available online 19 December 2012

Keywords:
Solid lubricant
Polymer nanocomposite
Transfer film
Low wear
PTFE

ABSTRACT

Polytetrafluoroethylene (PTFE) is an important solid lubricant with an unusually high wear rate. For a half-century, fillers have been used to reduce PTFE wear by $>100\times$ with $>10\%$ loading through hypothesized mechanisms involving mechanical load support, crack arresting, and transfer film adhesion. More recently it was discovered that specific nanoparticles provide a unique nanoscale reinforcement mechanism enabling unprecedented wear reductions of $10{,}000\times$ with as little as 0.1% nano-fillers. Although the mechanisms responsible for this dramatic improvement remain unclear, there is substantial evidence that the transfer film plays a critical role. This paper uses interrupted microscopy measurements to investigate the evolution of transfer film development for an ultra-low wear PTFE nanocomposite. The run-in wear rates were similar to those of more traditional PTFE composites and transfer films consisted of large plate-like debris. Although the run-in wear rate and debris size decreased monotonically with distance, the run-in transfer films were removed each cycle. Detectible debris vanished and wear rates approached zero at an abrupt transition. During this ultra-low wear transition period, nanoscale and oxidized fragments of PTFE were transferred to the counterface. Most of these fragments persisted for the duration of the test and initiated the transfer film by progressively scavenging trace material from the bulk, growing into small islands, and merging with neighboring islands. The results of this study reflect a complex interplay involving elements of transfer film adhesion, chemistry, debris morphology, and mechanics.

1. Introduction

Polytetrafluoroethylene (PTFE) is an important solid lubricant with a unique combination of beneficial frictional, thermal, and chemical properties. At sliding speeds well below 5 mm/s, PTFE friction coefficients are low ($\mu\sim0.05$) and wear rates are moderate ($k\sim10^{-5}$ mm^3/N m) [1–3]. The low friction of PTFE is often associated with low adhesion, but Makinson and Tabor [2] rejected this hypothesis based on the observation of molecularly thin, highly oriented, and strongly adhered transfer films following low friction sliding. They concluded that low friction results from easy shear of PTFE lamellae at low shear rates. At more typical speeds above 50 mm/s, friction coefficients are moderate ($\mu=0.15$–0.3), wear rates are high ($k\sim10^{-3}$ mm^3/N m), and transfer films consist of large platelets of poorly adhered debris fragments [2,4,5].

The addition of 20–50 wt% microscale fillers (e.g. glass fiber, carbon fiber, bronze particles) can reduce PTFE wear rates by >100 X at higher speeds [6–11]. However, large hard fillers can abrade protective transfer films which limits wear resistance. Nano-fillers have been studied for their potential to reduce wear without abrading the beneficial transfer film. Although an initial study by Tanaka and Kawakami indicated that nano-fillers were ineffective fillers because they were too small to disrupt the generation of large-scale debris [10], a series of studies from 2001 to 2003 showed that nanoscale ZnO, SWCNT's, and Al_2O_3 reduced wear rates by $>100\times$ at a fraction of the typical filler loading (5–10 wt%) [12–14]. In 2006, Burris and Sawyer [15] discovered a unique PTFE nanocomposite which demonstrated $>1000\times$ reductions in wear rates with $<1\%$ filler loading. This change in wear rate relative to the filler loading remains unprecedented in the field of tribological polymer nanocomposites today [16]. As a result, this particular material has been the subject of numerous follow-up studies of nanoscale polymer reinforcement mechanisms [17–23].

The role of the filler in preventing wear of PTFE and other polymer composites remains an important topic of debate. Blanchet and Kennedy [24] describe two general wear rate determining factors for PTFE composites: (1) the prevention of initial removal of material from the composite; (2) the prevention of the secondary removal of material from the transfer film. Lancaster proposed that fillers reduce primary wear of the matrix

* Corresponding author. Tel.: +1 302 831 2006.
E-mail address: dlburris@udel.edu (D.L. Burris).

0043-1648/$ - see front matter © 2012 Elsevier B.V. All rights reserved.
http://dx.doi.org/10.1016/j.wear.2012.12.002

by preferentially supporting the normal force [25]. Briscoe [26] proposed that fillers reduce secondary removal by inducing polymer degradation which increases adhesion between the transfer film and the counterface. Ricklin [27], Tanaka et al. [10], and Bahadur and Tabor [28] suggested similar mechanisms of primary wear reduction involving the prevention of large-scale debris generation. Blanchet and Kennedy supported this hypothesis and determined that the specific mechanism of debris size reduction involved the interruption of subsurface crack propagation [29]. Bahadur and Gong [30] made two overarching observations in reviewing the literature: (1) PTFE composite wear rate and filler hardness do not correlate as would be expected for the load support hypothesis; (2) wear rate is strongly dependent on filler chemistry which conflicts with the purely mechanical debris size regulation hypotheses. They supported Briscoe's hypothesis but concluded that filler decomposition rather than polymer degradation increases bonding to the counterface [30]. Gong et al. [31] and Blanchet et al. [24] showed that fillers had no effect on the chemistry at the counterface and independently concluded that the wear behavior is independent of counterface adhesion. Gong et al. [32] suggested that fillers served to improve transfer film cohesion and therefore reduce secondary wear by arresting failure within the transfer film. Blanchet et al. [24] note that severe wear of PTFE only occurs at high speeds and argues that the primary role of the filler must be most closely related to the prevention of primary removal [4,27,28]; this hypothesis is supported by two independent observations that pre-deposited low wear transfer films do not reduce the wear rate of high wear PTFE-based materials [28,33].

Despite opposing viewpoints about the specific wear reducing roles of filler decomposition, polymer degradation, transfer film adhesion, and transfer film cohesion, there is a broad agreement that transfer films play a very important role in the tribology of polymers. Thin and uniform transfer films always accompany low wear sliding of polymers and transfer film adhesion arguments persist today as a causative explanation for low wear rates [34–36]. The purpose of the present study is to elucidate the relationships between wear rate, debris size, and transfer film morphology via direct *in situ* observations of debris generation and transfer film formation. A well-documented PTFE-alumina nanocomposite was chosen as a model of effective reinforcement due to its exceptional wear reduction with low filler loading [17–20].

2. Materials and methods

2.1. Materials

The PTFE nanocomposite materials used in this study replicate, as closely as possible, the preparation conditions from existing literature [15,17–20,37]. The polymer resin is Teflon™ 7C from DuPont (~30 μm diameter particles). The alpha phase aluminum oxide nanoparticles had a reported diameter range of 27–43 nm and were acquired from Nanostructured & Amorphous Materials Inc.[1]

2.2. Sample preparation

Aluminum oxide nanoparticles and polytetrafluoroethylene resin were weighed to 0.5 g and 9.5 g, respectively, combined in a PET container of 10 times the batch volume and pre-mixed by hand shaking for 60 s. The powder ensemble was suspended in 80 mL of anhydrous ethanol which wets PTFE reasonable well [38]. An ultrasonic horn (Sonic Ruptor 400, OMNI International) was pulsed with a 50% duty cycle of 400 W for 5 min. Immediately after ultrasonication, the suspension was transferred to a petri dish placed within a heated vacuum desiccator. Two hours of rough vacuum drying at 110 °C removed the ethanol and prepared the dispersed nanocomposite resin for subsequent compression molding. The dry powder was cold pressed into a 25 mm long, 12.5 mm diameter cylinder using a cylindrical die. Each preform was held at a pressure of 170 MPa for 20 min to eliminate porosity. Following cold compaction, samples were held at 6 MPa pressure and heated to 365 °C at 120 °C per hour, held for 3 h, and cooled at the same rate.

2.3. Wear testing

Prior to testing, each cylindrical specimen was machined into a pin of 6.4 × 6.4 mm testing cross-section and 12 mm height. Grade 304 stainless steel plates (38 × 25 mm) with an average surface roughness of 20 nm (R_a) were used as counterfaces. Wear tests were conducted on the linear reciprocating pin-on-flat tribometer shown in Fig. 1; the tribometer is nominally identical to those reported in previous studies [15,37]. Prior to testing, the sample was preconditioned with 100 mm of sliding at 0.7 MPa of pressure against 600 grit SiC paper to create a uniform pressure distribution for testing. During the test, the applied normal force was 250 N, the contact pressure was 6.4 MPa, the reciprocating length (one direction) was 25.4 mm, and the sliding speed was 50 mm/s. Initial length and mass measurements were used to determine sample density. Mass measurements were then used to quantify mass loss; the volume loss is the ratio of mass loss and density. Friction coefficients, wear rates, and uncertainties were determined using previously described methods [39–41].

Tests were interrupted periodically for analysis. Following interruption, the sample was removed from the mounting fixture and weighed on a balance with a resolution of 0.01 mg. The counterface was removed and located on a kinematic mount beneath a Nikon microscope with a digital camera. Images were captured at a single location in the center of the counterface to follow the morphological evolution of the transfer film. The primary test was interrupted every few cycles to capture the details of the run-in process; interruption intervals increased as the distance between distinct events at the interface increased. Repeat tests with three independent samples were conducted with less frequent interruptions to determine repeatability and the effects of test interruption interval on the results.

3. Results

3.1. Wear behavior of α-aluminum oxide PTFE nanocomposites

This PTFE nanocomposite material is known to exhibit a transient period of moderate wear followed by a transition to a low steady state wear rate [15]. A mass loss measurement taken after 0.2 m revealed an initial wear rate of $k = 4 \times 10^{-4}$ mm^3/N m. This high initial wear rate suggests that the direct mechanical reinforcement effect of the nanoparticles (e.g. preferential load support, crazing, crack arresting) is initially limited. Wear volume is plotted as a function of sliding distance for the first 300 m of the primary test in Fig. 2a. There is an obvious run-in period during the first 20 m of sliding where the wear rate decreases monotonically with distance. The wear rate at the end of the run-in period is typical of other PTFE composites and nanocomposites

[1] It is important to note that only particular alpha phase alumina particles activate the ultra-low wear response of interest in this paper. The initiating mechanism likely involves surface-chemistry (and history) dependent interactions between particle and polymer. Prior studies used 27–43 nm particle from Alfa Aesar which are no longer available. Efforts to locate a suitable surrogate demonstrated wide variability in wear rates between suppliers. The particles in this study exhibited the same wear response and have the same reported size range.

at $k=6\times10^{-6}$mm^3/N m. An abrupt transition in wear rate occurred at 20 m and the mass loss over the next 145 m was at the resolution of the scale (10 μg). This nearly zero-wear period is referred to here as the transition period. This behavior is repeatable as nearly identical features were observed in the five preliminary measurements used to develop the experimental protocols for this paper (preliminary results not shown). The wear increased at 165 m and the system reached steady-state at a wear rate of $k=2\times10^{-7}$ mm^3/N m shortly thereafter.

Comparative plots of friction coefficient and wear volume for primary and repeat tests are shown in Fig. 2b. The three repeat tests exhibit similar trends in their evolutions of friction coefficient and wear rate indicating that the general tribological features are characteristics of this system. A comparison between primary and repeat test results indicates that the test interruptions had a significant friction reducing effect. Oxidation accompanies decreased wear and leads to increased friction as shown in the discussion. A series of follow-up experiments suggested that ambient moisture passivates the oxidized surfaces during interruptions and subsequently reduces friction. The wear rate on the other hand was unaffected by the high frequency test interruptions. Although the wear response of this material has not been documented previously at this level of detail, the general run-in and steady-state responses are consistent with the results in the literature. The characteristic features of this tribo-system are discussed in the context of transfer film evolution in the following sections.

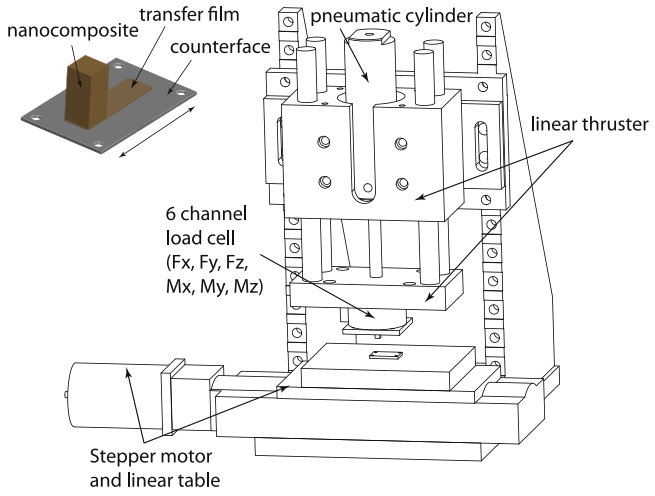

Fig. 1. Pin on flat tribometer used for friction and wear testing. A flat pin of the bulk nanocomposite is loaded (6.3 MPa, 250 N) against a linearly reciprocating 304 stainless steel counterface with an average roughness of R_a=20 nm. A six-channel load cell is used to measure normal and frictional forces during the test. The sliding speed is 50.8 mm/s and the reciprocation cycle is 50.8 mm long.

3.2. Transfer film development

In situ observations of the transfer film evolution revealed three unique transfer film morphologies; these are used to define the *run-in*, *transition*, and *steady-state* sliding periods. Representative optical images of the transfer film in each period are shown in Fig. 3.

During the high wear *run-in* period, the transfer film comprises large plate-like debris not unlike those characterizing the delamination wear of PTFE and some of its composites. Plates have in-plane dimensions of 100–500 μm as compared to 1–5 mm for neat PTFE suggesting that the nanoparticles do compartmentalize damage after only a few meters of sliding. In the *transition* period, the transfer film is extremely thin and shows no evidence of loosely adhered debris. In the low wear *steady-state* period, the transfer film has an island-like morphology.

3.3. Run-in period

Images of the transfer film during the *run-in* period are shown in Fig. 4 after 2.4, 4.6, 6.1, and 8.1 m of sliding. After 4.6 m of sliding, the transfer film consists of large plate-like debris showing evidence of tearing and fibrillation at the debris edges. In some cases, especially early in the test, debris were layered (left side, 2.4 m). Transferred material only rarely remained for multiple passes; therefore, the transfer film reflects the wear debris. During this period, the debris were generated, deformed by the contact, left behind, removed, and replenished. Debris size and wear rate decreased as distance increased. This data supports a previous

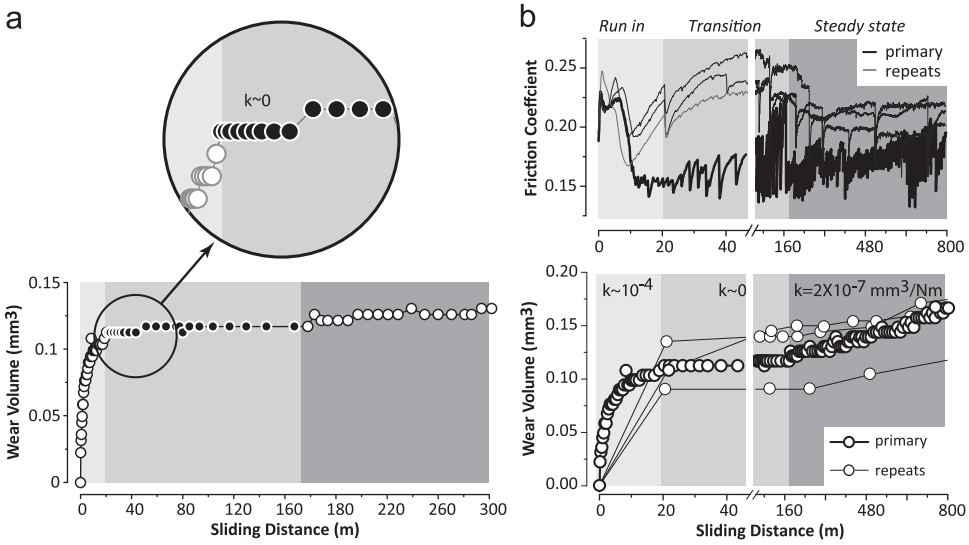

Fig. 2. (a) Wear volume versus sliding distance for the first 300 m of the sliding experiment. The initial wear rate was $k=4\times10^{-4}$ mm^3/N m. The wear rate decreased monotonically over the next 20 m; this is referred to here as the *run-in* phase. The mass loss in the following *transition* phase was at the 10 μg resolution limit of the scale. The transition phase is highlighted by black data labels (a). (b) Friction coefficient and wear volume plotted versus sliding distance for the primary measurement with high frequency interruptions and repeat measurements with more typical interruption frequency (800 m of sliding). At *steady-state*, the wear rate was $k=2\times10^{-7}$ mm^3/N m. Friction coefficient was reduced by high interruption frequency while the wear behavior was nominally unaffected.

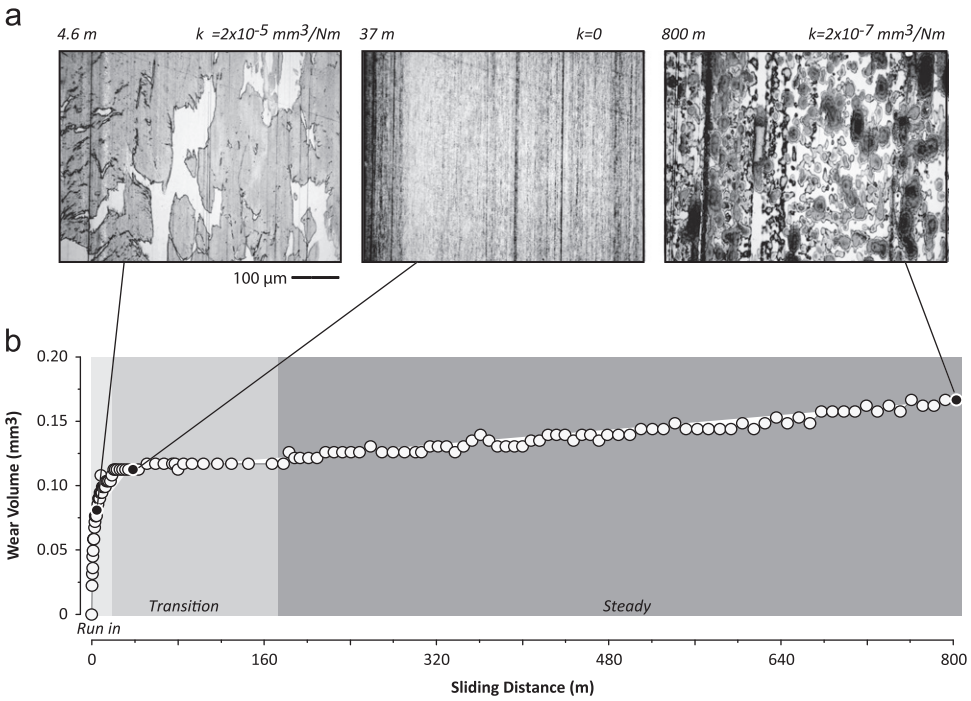

Fig. 3. (a) Representative images of the transfer film morphology for the run-in, transition, and steady-state phases. The stainless counterface appears bright. (b) Wear volume is plotted versus distance for the first 800 m of sliding. The images correspond to the black data labels. Each image has the scale shown.

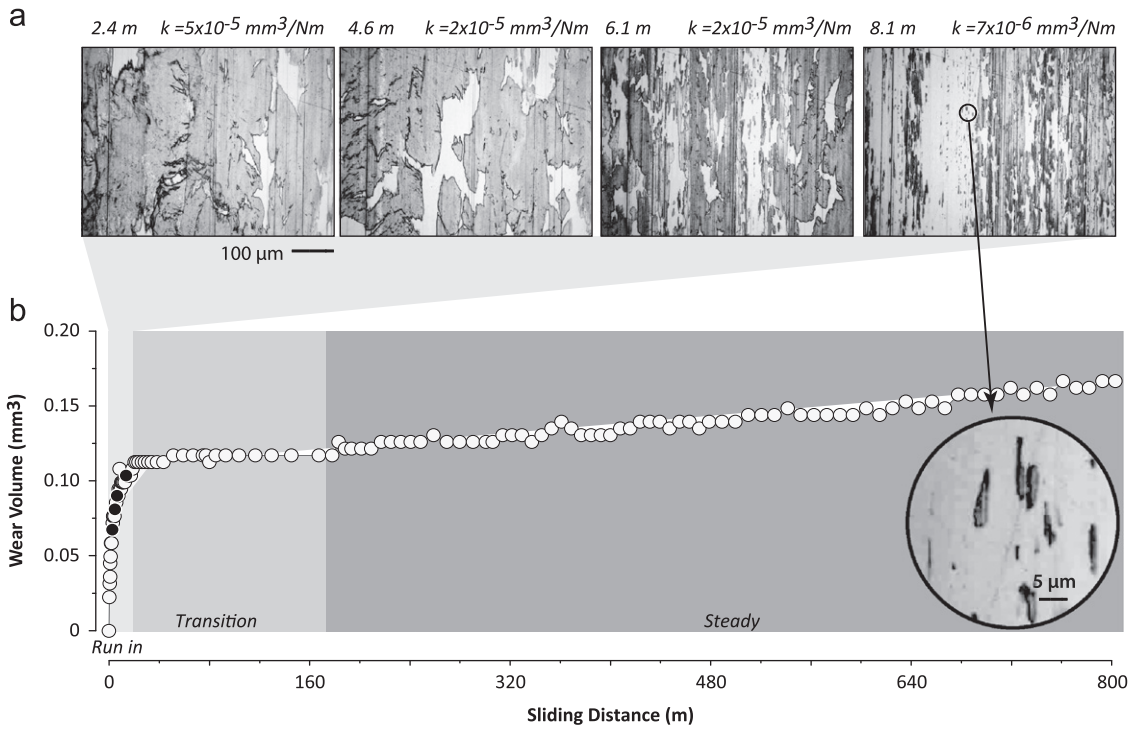

Fig. 4. (a) Images showing the transfer film development at a single location during the run in period; (b) wear volume versus distance for the first 800 m. Images correspond to the black data labels.

hypothesis that reduced debris size causes transfer film thinning [33]. It is not clear, however, to what extent thin transfer films affect debris size; clearly there is an opportunity for positive feedback between reduced film thickness and reduced debris size. At 8.1 m, debris within the film were as small as a few microns and wear rates are similar to those of more typical PTFE composite and nanocomposite materials.

3.4. Transition period

Images of the transfer film during the *transition* period are shown in Fig. 5. The *transition* period is characterized by the absence of the loose debris characterizing the *run-in* transfer film. The wear rate abruptly decreased in the transition period and maintained a value of $k=1.2\times10^{-8}$ mm^3/N m $\pm k=2.4\times10^{-7}$ mm^3/N m.

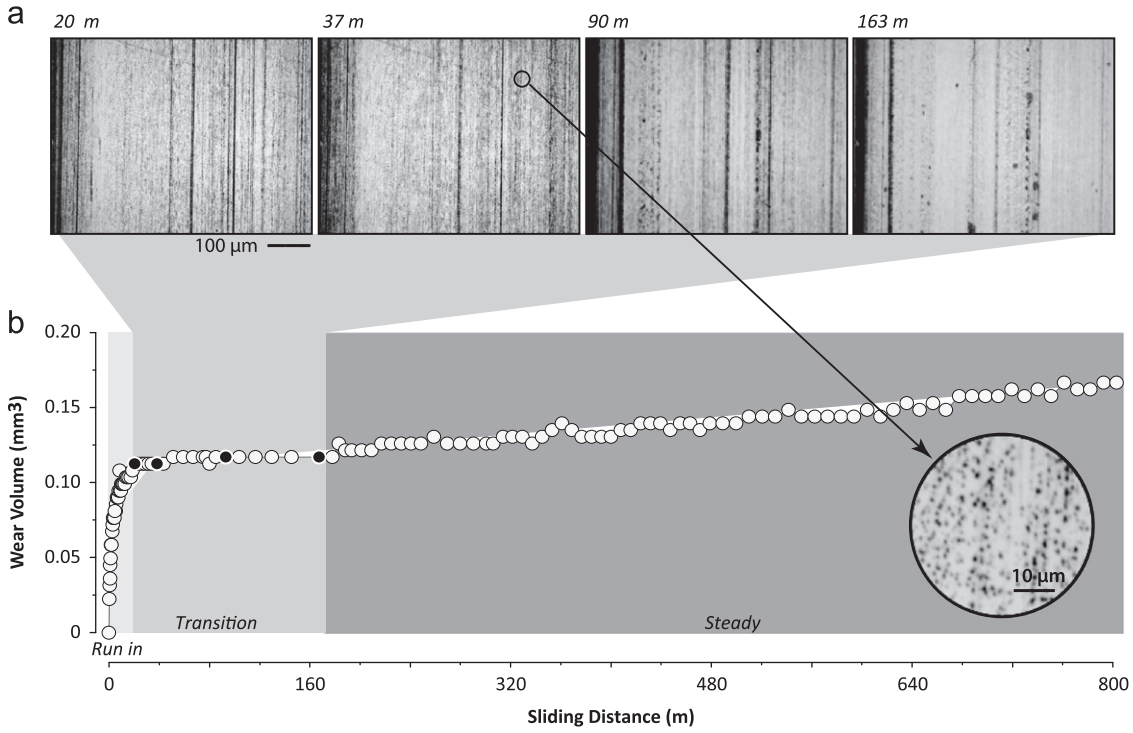

Fig. 5. (a) Representative images of the transfer film morphology during the transition period. Higher resolution imaging reveals that the film consists of discrete regions of transferred material. AFM imaging reveals that the regions have submicron lateral dimensions and are 5–10 nm thick. (b) Wear volume versus distance for the first 800 m. Images correspond to the black data labels.

Electron and atomic force microscopy revealed that the film comprises discrete regions of transferred material with 100–1000 nm width and 5–10 nm height, respectively; we call these regions seeds because they appear to nucleate the transfer film. In stark contrast to the single cycle residence time of transferred material in the *run-in* period, the residence time of a seed appears to be the length of the test with seed removal being a rare event. The film darkened over time due to an increase in the size and number density of the seeds.

3.5. Steady-state period

Images of the transfer film during the *steady state* period are shown in Fig. 6. At 172 m, a thick streaked transfer film comprising small islands with lateral dimensions of ~1–20 µm was deposited suddenly. Interestingly, this initial event occurred in the absence of detectable mass loss (163 m and 172 m, Fig. 5). However, this thicker film appeared to initiate the transition to steady state as significant mass loss was observed on the next measurement (178 m, Fig. 5). The wear rate remained steady for the remainder of the test at 2×10^{-7} mm^3/N m, a value that is an order of magnitude or more lower than that of a typical PTFE composite or nanocomposite at the same conditions. These films were tenacious, persisting for the entire test in most areas. At 525 m of sliding, the film covered a larger fraction of the view field and exhibited an island-like morphology with islands being in the 20–50 µm range. At 800 m the island size and density increased. The transfer film was nearly continuous at 5600 m.

The details of the steady-state transfer film development process are illustrated in Fig. 7. Initiating seeds and the beginnings of the transfer film are visible at 485 m. At 505 m, the seeds remained well adhered and enlarged in some cases. At 515 m, the growth process continued, clearly distinguishing the evolution in the *steady-state* phase as a nucleation and growth process as opposed to the direct debris deposition process characterizing the *run-in* phase. At 536 m the growing seeds merge into a single island. These islands have very long residence times; they remain well adhered, grow with distance, connect with other islands, and eventually form a continuous transfer film as shown in Fig. 6a.

4. Discussion

The high initial wear rates suggest that 2.5% nanoparticles provides negligible preferential load support [42] and debris size regulation [10,28,29]. Additionally, transfer films were removed by each pass of the pin which suggests that wear rate was unaffected by any potential benefits of improved transfer film adhesion [26,30] or cohesion [32]. Energy dispersive x-ray spectroscopy (EDX) and nano-indentation measurements (Fig. 8) showed that the composition and mechanical properties of the *run-in* transfer film were indistinguishable from those of the bulk. The wear rate and debris size decreased monotonically with increased sliding distance in the run-in phase (Fig. 4) despite the fact that the transfer film was completely removed and replenished with each pass. Therefore, the reduction in wear with increased sliding was due to a reduction in primary removal (reduced debris size) not to a reduction in secondary removal (transfer film adhesion and cohesion). Interestingly, debris regulation and the responsible properties improved over time. Compact tensile tests (unpublished) have shown that these low wear PTFE nanocomposites have a unique fibrillation response to stress concentration at a sharp crack (neat PTFE blunts but doesn't fibrillate). Extensive fibrillation has also been observed on worn pins and transfer films [16,21,33]. Easy fibrillation at subsurface crack tips may interrupt crack propagation, substantially change the mechanical properties of the near surface polymer, and improve debris size regulation with increased sliding distance. The lack of oxidation and poor residence time of run-in transfer films suggest that the nanoparticles did not directly induce polymer degradation [30], enhance counterface adhesion [26,30], or enhance wear resistance through transfer film cohesion [31,32].

The *transition* period is characterized by nanoscale debris fragments which appear to nucleate the transfer film; unlike *run-in*

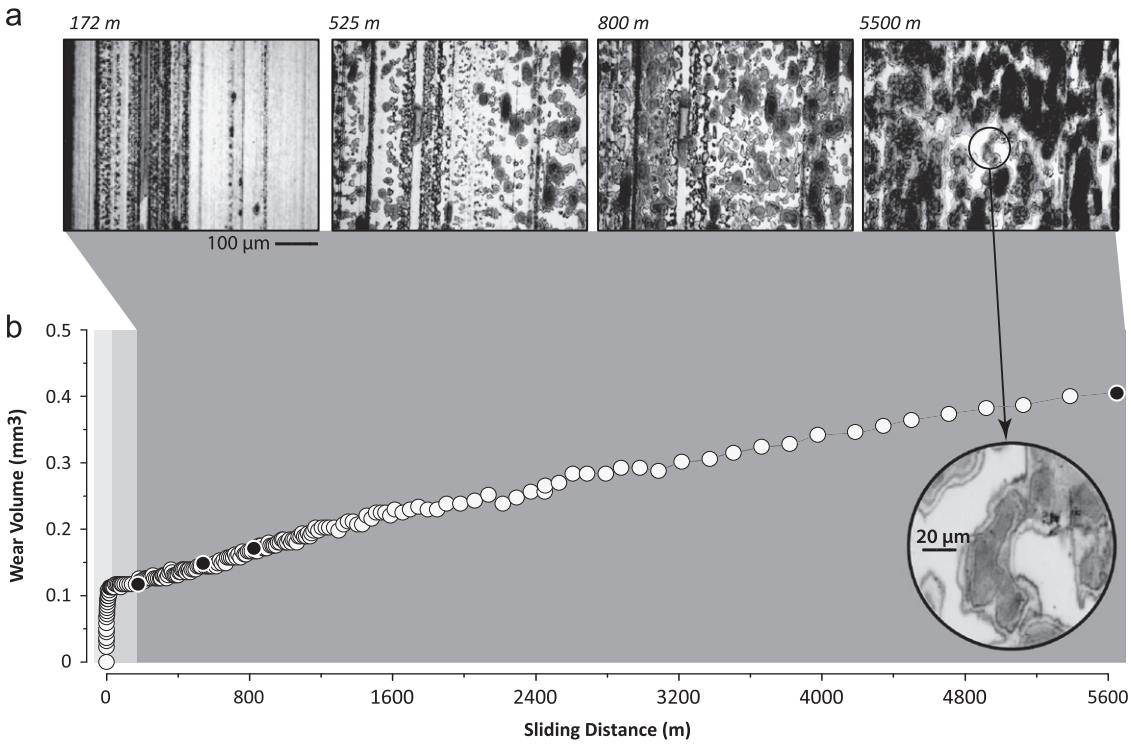

Fig. 6. (a) Representative images of the transfer film morphology during the steady state period. (b) Wear volume versus distance. Images correspond to the black data labels.

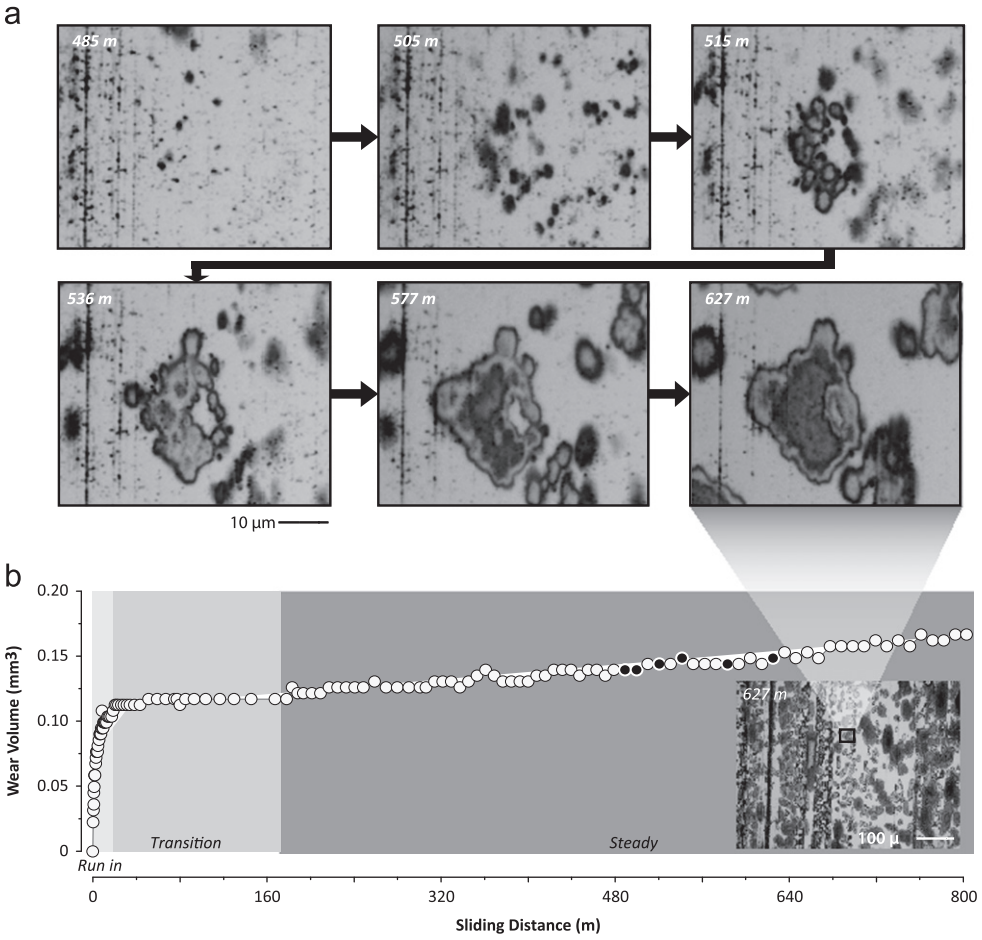

Fig. 7. (a) Images showing the "seed-growing" process for one island within the transfer film; (b) corresponding data points on the wear curve.

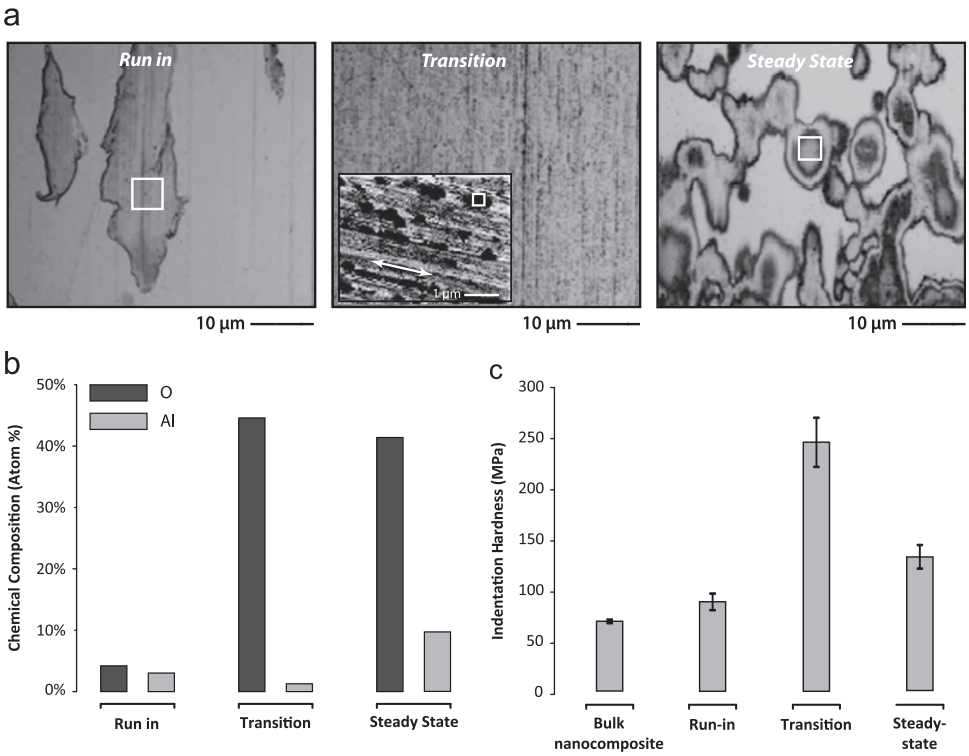

Fig. 8. (a) Images showing transfer film's characteristic feature at different periods; (b) EDX analysis of the oxygen and aluminum content at different stages. The aluminum reflects filler contributions while oxygen reflects de-fluorination and oxidation of the PTFE. (c) Film hardness at different stages measured using atomic force microscopy (AFM). Hardness was calculated as force over projected contact area. The bulk nanocomposite is shown for reference. Each data set contains at least 15 independent measurements and error bars represent statistical 95% confidence intervals. There are significant increases in oxidation and hardness during the test (substrate effects were present during transition hardness measurements and artificially increased the magnitude).

films, *transition* films were extremely well adhered. EDX results show little evidence of aluminum which suggests that filler accumulation and preferential load support were not responsible for the gradual reduction in wear or the abrupt transition to low wear [43]. Further, it shows that alumina was not directly involved in anchoring the seeds to the counterface. Rather, EDX (Fig. 8b) demonstrates that the PTFE-rich transition film is highly oxidized in accordance with Briscoe's transfer film adhesion hypothesis. However, given the lack of oxidation following sintering at 362 °C and high wear sliding, it can be concluded that the alumina nanoparticles did not directly induce polymer degradation. Prior XPS studies of this system have demonstrated de-fluorination, conjugation, and oxidation of PTFE during low wear sliding. The results consistently suggest that the residence time of the interface becomes sufficiently long (due to ultra-low wear rates) that frictional energy initiates the degradation process; this is interesting given the low temperatures involved and the notable inertness of the polymer. Polymer degradation promotes adhesion while transfer film continuity and thinness reduces the mechanical interaction with the pin. The results suggest that debris size, transfer film uniformity, and residence time feedback positively to initiate the abrupt decrease in wear rate and the increase in transfer film residence time. At *steady state*, the transfer film remains extremely stable, highly oxidized, and harder than the parent nanocomposite. A significant increase in aluminum content suggests accumulation of the filler [43]. While the role of filler accumulation is unclear, it does not appear to be a primary mechanism of wear reduction for this system.

Thin continuous transfer films consistently accompany low wear sliding of polymers. Previous studies have shown that the wear rate correlates strongly with transfer film thickness [37,44]. One of the greatest remaining questions is whether thin well-adhered transfer films are the *cause* of low wear or the *consequence* of low wear. The results of this study show that there is a coupling of debris size and transfer film morphology but they provide little direct insight into the cause and effect relationship leading to the transition to low wear. One clue comes from the fact that the transfer film accumulated mass while the pin lost mass at steady-state. Thus, primary wear occurs with or without secondary wear; this explains the observation that pre-deposited low wear transfer films do not reduce the wear rate of unfilled PTFE or high wear nanocomposites [28,33]. We interrupted the steady state test and replaced the worn pin with a fresh pin. Interestingly, the presence of the low wear transfer film actually increased the initial wear rate and the volume lost before reaching steady state. Thus, the low wear transfer film is insufficient for low wear in agreement with observations from Bahadur and Tabor [28] and Burris et al. [33]. Next, a worn pin was slid against a fresh counterface to determine if the transfer film is necessary to sustain low wear. The initial wear rate was $100\times$ lower (2×10^{-6} $mm^3/N\,m$) and quickly dropped another order of magnitude once the transfer film reformed to restore steady-state conditions. Thus, while low wear transfer films are necessary for low wear sliding, the mechanics of the near surface region and the regulation of debris are primarily responsible for ultra-low wear rates in this material system.

5. Conclusion

1. Three distinct transfer film morphologies define the sliding regimes and wear response of an ultra-low wear PTFE nanocomposite: run-in, transition, and steady state.
2. In the run-in period, debris are chemically and mechanically identical to the bulk. They are generated, transferred, and quickly removed from the counterface. Debris size, transfer

film thickness, and wear rate decrease monotonically despite poor adhesion and residence time of transfer films.

3. The transition period is denoted by the sudden absence of gross mass loss and poorly adhered debris, and the presence of a transfer film comprising 20 nm thick seeds of highly oxidized PTFE with long residence times. The transition period appears to begin at a point when debris size and adhesion are sufficient to survive multiple passes of the pin without removal.
4. The steady state period begins with the deposition of small islands of oxidized debris ($\sim$1 μm in diameter). These islands are persistent and grow radially with increased sliding by progressively scavenging material from the bulk. Over time, individual islands meet, merge, and form a continuous transfer film.
5. The filler does not play a direct role in promoting adhesion of the transfer film. The filler appears to change the mechanical response of the polymer to concentrated stresses. A progressive reduction in debris size reduces the wear rate and increases residence times of the surfaces. Debris size, residence times of surfaces, polymer degradation, and adhesion are interrelated.
6. The transfer film does not cause low wear; it evolves in response to the wear debris morphology and chemistry.

Acknowledgments

The authors gratefully acknowledge financial support from the AFOSR (YIP FA9550-10-1–0295) for financial support of this work.

References

[1] D. Breiby, et al., Structural surprises in friction-deposited films of poly(tetrafluoroethylene), Macromolecules 38 (6) (2005) 2383–2390.
[2] K. Makinson, D. Tabor, The friction and transfer of polytetrafluoroethylene, Proceedings of the Royal Society of London Series A 281 (1384) (August 1964) 49–61.
[3] C. Pooley, D. Tabor, Friction and molecular structure – behavior of some thermoplastics, Proceedings of the Royal Society of London Series A: Mathematical and Physical Sciences 329 (1578) (1972) 251–274.
[4] T.A. Blanchet, F.E. Kennedy, Sliding wear mechanism of polytetrafluoroethylene (PTFE) and PTFE composites, Wear 153 (1) (1992) 229–243.
[5] K. Tanaka, Y. Uchiyama, S. Toyooka, The mechanism of wear of polytetrafluoroethylene, Wear 23 (2) (1973) 153–172.
[6] S. Bahadur, D. Tabor, The wear of filled polytetrafluoroethylene, Wear 98 (1–3) (1984) 1–13.
[7] J. Khedkar, I. Negulescu, E. Meletis, Sliding wear behavior of PTFE composites, Wear 252 (5–6) (2002) 361–369.
[8] B. Menzel, T. Blanchet, Effect of particle size and volume fraction of irradiated FEP filler on the transfer wear of PTFE, Lubrication Engineering 58 (9) (2002) 29–35.
[9] N. Sung, N. Suh, Effect of fiber orientation on friction and wear of fiber reinforced polymeric composites, Wear 53 (1) (1979) 129–141.
[10] K. Tanaka, S. Kawakami, Effect of various fillers on the friction and wear of polytetrafluoroethylene-based composites, Wear 79 (2) (1982) 221–234.
[11] T. Blanchet, Y. Peng, Wear resistant irradiated FEP unirradiated PTFE composites, Wear 214 (2) (1998) 186–191.
[12] W. Chen, et al., Tribological behavior of carbon-nanotube-filled PTFE composites, Tribology Letters 15 (3) (2003) 275–278.
[13] F. Li, et al., The friction and wear characteristics of nanometer ZnO filled polytetrafluoroethylene, Wear 249 (10–11) (2001) 877–882.
[14] W. Sawyer, et al., A study on the friction and wear behavior of PTFE filled with alumina nanoparticles, Wear 254 (5–6) (2003) 573–580.
[15] D. Burris, W. Sawyer, Improved wear resistance in alumina-PTFE nanocomposites with irregular shaped nanoparticles, Wear 260 (7–8) (2006) 915–918.
[16] D.L. Burris, et al., Polymeric nanocomposites for tribological applications, Macromolecular Materials and Engineering 292 (4) (2007) 387–402.
[17] S.S. Kandanur, et al., Suppression of wear in graphene polymer composites, Carbon 50 (9) (2012) 3178–3183.
[18] S. McElwain, et al., Effect of particle size on the wear resistance of alumina-filled PTFE micro- and nanocomposites, Tribology Transactions 51 (3) (2008) 247–253.
[19] D.L. Burris, et al., A route to wear resistant PTFE via trace loadings of functionalized nanofillers, Wear 267 (1–4) (2009) 653–660.
[20] B.A. Krick, et al., Environmental dependence of ultra-low wear behavior of polytetrafluoroethylene (PTFE) and alumina composites suggests tribochemical mechanisms, Tribology International (2012) 42–4651 (2012) 42–46.
[21] S.E. McElwain, Wear Resistant PTFE Composites via Nano-Scale Particles, Rensselaer Polytechnic Institute, Troy, NY, 2006.
[22] D.L. Burris, Effects of nanoparticles on the wear resistance of polytetrafluoroethylene, Mechanical Engineering, University of Florida, Gainesville, FL, 2007.
[23] S.S. Kandanur, The role of filler size & content and countersurface roughness in the wear resistance of alumina-PTFE nano-composites, Rensselaer Polytechnic Institute, Troy, NY, 2010.
[24] T. Blanchet, F. Kennedy, D. Jayne, XPS analysis of the effect of fillers on PTFE transfer film development in sliding contacts, Tribology Transactions 36 (4) (1993) 535–544.
[25] J.K. Lancaster, Polymer-based bearing materials – role of fillers and fiber reinforcement in wear, wear 22 (3) (1972) 412–413.
[26] B. Briscoe, Wear of polymers – an essay on fundamental-aspects, Tribology International 14 (4) (1981) 231–243.
[27] S. Ricklin, Review of design parameters for filled PTFE bearing materials, Lubrication Engineering 33 (9) (1977) 487–490.
[28] S. Bahadur, D. Tabor, The wear of filled polytetrafluoroethylene, Wear 98 (1984) 1–13.
[29] T. Blanchet, F. Kennedy, Sliding wear mechanism of polytetrafluoroethylene (PTFE) and PTFE composites, Wear 153 (1) (1992) 229–243.
[30] S. Bahadur, D. Gong, The action of fillers in the modification of the tribological behavior of polymers, Wear 158 (1–2) (1992) 41–59.
[31] D. Gong, Q. Xue, H. Wang, ESCA study on tribochemical characteristics of filled PTFE, Wear 148 (1) (1991) 161–169.
[32] D. Gong, Q.J. Xue, H.L. Wang, Physical models of adhesive wear of polytetrafluoroethylene and its composites, Wear 147 (1) (1991) 9–24.
[33] D.L. Burris, et al., Polytetrafluoroethylene matrix nanocomposites for tribological applications, in: K. Friedrich, A.K. Schlarb (Eds.), Tribology of polymeric nanocomposites, 2010, pp. 403–438.
[34] S. Bahadur, C. Sunkara, Effect of transfer film structure, composition and bonding on the tribological behavior of polyphenylene sulfide filled with nano particles of TiO_2, ZnO, CuO and SiC, Wear 258 (9) (2005) 1411–1421.
[35] M.H. Cho, S. Bahadur, A.K. Pogosian, Friction and wear studies using Taguchi method on polyphenylene sulfide filled with a complex mixture of MoS2, Al2O3, and other compounds, Wear 258 (11–12) (2005) 1825–1835.
[36] A. Dasari, Z.Z. Yu, Y.W. Mai, Fundamental aspects and recent progress on wear/scratch damage in polymer nanocomposites, Materials Science and Engineering R: Reports 63 (2) (2009) 31–80.
[37] D. Burris, W. Sawyer, Tribological sensitivity of PTFE/alumina nanocomposites to a range of traditional surface finishes, Tribology Transactions 48 (2) (2005) 147–153.
[38] L.X. Shi, et al., Wetting and evaporation behaviors of water–ethanol sessile drops on PTFE surfaces, Surface and Interface Analysis 41 (12-13) (2009) 951–955.
[39] D.L. Burris, W.G. Sawyer, Measurement uncertainties in wear rates, Tribology Letters 36 (1) (2009) 81–87.
[40] D.L. Burris, W.G. Sawyer, Addressing practical challenges of low friction coefficient measurements, Tribology Letters 35 (1) (2009) 17–23.
[41] T. Schmitz, et al., The difficulty of measuring low friction: uncertainty analysis for friction coefficient measurements, Journal of Tribology – Transactions of the ASME 127 (3) (2005) 673–678.
[42] J.K. Lancaster, Polymer-based bearing materials: the role of fillers and fibre reinforcement, Tribology 5 (6) (1972) 249–255.
[43] T.A. Blanchet, A model for polymer composite wear behavior including preferential load support and surface accumulation of filler particulates, Tribology Transactions 38 (4) (1995) 821–828.
[44] T.A. Blanchet, S.S. Kandanur, L.S. Schadler, Coupled effect of filler content and counter surface roughness on PTFE nanocomposite wear resistance, Tribology Letters 40 (1) (2009) 11–21.